

Proximity effect thermometer for local electron temperature measurements on mesoscopic samples

J. Aumentado and V. Chandrasekhar^{a)}

Department of Physics and Astronomy, Northwestern University, Evanston, Illinois 60208

J. Eom

The James Franck Institute and Department of Physics, University of Chicago, Chicago, Illinois 60637

P. M. Baldo and L. E. Rehn

Materials Science Division, Argonne National Laboratory, Argonne, Illinois 60439

(Received 19 April 1999; accepted for publication 6 October 1999)

Using the strong temperature-dependent resistance of a normal metal wire in proximity to a superconductor, we have been able to measure the local temperature of electrons heated by flowing a direct-current (dc) in a metallic wire to within a few tens of millikelvin at low temperatures. By placing two such thermometers at different parts of a sample, we have been able to measure the temperature difference induced by a dc flowing in the samples. This technique may provide a flexible means of making quantitative thermal and thermoelectric measurements on mesoscopic metallic samples. © 1999 American Institute of Physics. [S0003-6951(99)04648-3]

For many experiments on mesoscopic metallic samples, the issue of determining the effective temperature T_e of the electrons at low temperature is of critical importance. This is because it is T_e which determines the electronic properties of the system, and not the temperature T_b of the thermal bath in which the sample is placed. With an energy input into the electron gas, the difference between T_e and T_b can be large, particularly at low temperatures, where the rapid decrease in the electron-phonon interaction means that the electron gas is out of equilibrium with the phonon bath. Hence it is not possible to determine the electron temperature by conventional low temperature thermometers (which are typically well coupled only to the phonon bath), and the need arises for thermometers which directly measure the electron temperature.

In samples whose dimensions are much shorter than the electron-electron scattering length L_{ee} , the electron system itself may not be in equilibrium, so that the question of the effective electron temperature is not a valid one. This was elegantly demonstrated in a recent experiment by Pothier *et al.*,¹ who measured the nonequilibrium electron distribution function in a short metal wire using mesoscopic superconductor-insulator-normal metal (SIN) junctions. For samples whose dimensions are longer than L_{ee} but shorter than the electron-phonon scattering length L_{ep} , however, one can think about a position dependent local electronic temperature T_e which can be substantially different from T_b .² Previous techniques to measure T_e have included correlating the temperature with the Johnson noise measured across a sample,²⁻⁴ utilizing the temperature dependence of the weak localization contribution to the magnetoresistance,⁵ or measuring the current voltage characteristics of a metallic system weakly coupled to a superconductor.¹

In this letter, we describe a thermometer which makes use of the large temperature dependent resistance of the su-

perconducting proximity effect to measure the temperature at different points of a complex mesoscopic sample. In contrast to techniques utilizing noise measurements or weak localization, which only measure the average temperature over relatively long samples, this thermometer can measure the electron temperature over size scales as small as ~ 100 nm. Consequently, one can determine the gradient of the electron temperature in a mesoscopic sample, which may prove useful in making *quantitative* thermal and thermoelectric measurements on mesoscopic samples.

The samples for this experiment were fabricated using standard multilevel electron beam lithography techniques. Figure 1 shows a scanning electron micrograph of one of our samples. The design of the samples was driven by our ongoing experiments on the width dependence of the thermopower in mesoscopic Kondo wires,⁶ which will be described in detail elsewhere. The bright regions in the micrograph of Fig. 1(a) correspond to a 51-nm-thick Au film which was deposited in the first level of lithography. After

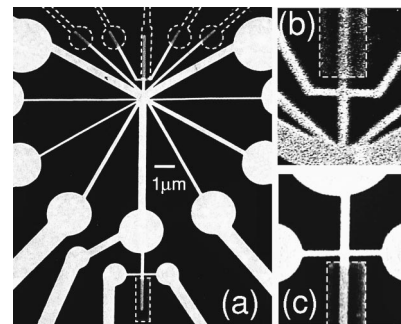


FIG. 1. Scanning electron microscopy (SEM) images of device structure. (a) Large area layout. Al structures are outlined with dashed lines for clarity. The wide V-shaped wire with contacts marked $I_{dc}\pm$ which runs left to right at the top is the heater. (b) and (c) are closeup views of the top and bottom thermometers, respectively. The resistance of the vertical segments is measured using the other wires in a four-terminal configuration.

^{a)}Electronic mail: v-chandrasekhar@nwu.edu

implantation of this entire layer with Fe ions to a concentration of ~ 100 ppm,⁷ a 75-nm-thick Al film was deposited to form the proximity effect thermometers (the Al film is outlined by dashed white lines for clarity). The sample consists of a number of wires which meet at a central node. The 0.36- μm -wide V-shaped wire at the top of Fig. 1(a) is the heater wire through which a dc current can be driven to raise the effective temperature T_e of the electrons at the node above the bath temperature T_b . From the node, seven wires of different widths radiate downward, each terminating in a large circular pad. These are the samples for the width-dependent Kondo thermopower experiment, and they include a 0.38- μm -wide reference wire which runs vertically from the node to a circular pad at the bottom of the micrograph. The heat transport along all of these radial wires is a function of width and Fe impurity concentration,⁶ and each may support different temperature gradients along their lengths.

In this sample, there are two proximity effect thermometers which are shown in greater detail in Figs. 1(b) and 1(c). The first, which we will denote the top thermometer [Fig. 1(b)], is attached to the top of the node. It consists of a ~ 0.5 - μm -long AuFe wire with five terminals. One terminal is connected to an Al film which provides the superconducting reservoir for the proximity effect. The remaining contacts are used for making four terminal resistance measurements on the wire. These contacts are connected to the wire bonding pads by superconducting Al lines. The Al has negligible thermal conductivity below $T \sim T_c/2$ (we estimate the Al thermal conductivity to be $\sim 1\%$ of the Au value at $T \sim 340$ mK). This ensures that heat loss through these contacts is minimized, and consequently, the thermal gradient across the length of the thermometer is small. The normal metal part of the thermometer, which is evaporated at the same time as the heater, is well coupled thermally to the node.

The second thermometer, which we denote the bottom thermometer [Fig. 1(c)], is attached to the circular terminal pad of the wide reference wire. This thermometer is ~ 1.0 μm long, and can also be measured using four terminals, two of which are connected through the circular pad. One dangling lead connected to the thermometer terminates in an Al film, which provides the superconducting reservoir for the proximity effect for this thermometer. In this geometry, we expect that the presence of a dc current in our heater wire will create a temperature gradient along the reference wire, raising the temperature measured by the top thermometer above that measured at the bottom. It should be noted that for both thermometers, the four-terminal resistance does not include the Al film, but only the proximity coupled normal metal. Because the heater consists of a single wire which spans a distance of 40–50 μm between large photolithographed pads, we expect the system to be in a regime where electrons may locally thermalize as indicated by previous experiments which measured local electron Fermi distributions.¹

The proximity effect thermometers were first calibrated against a RuO₂ thermometer attached to the mixing chamber of a dilution refrigerator by measuring the resistance of the thermometers as a function of temperature with no dc current flowing through the sample. The resistance of the thermom-

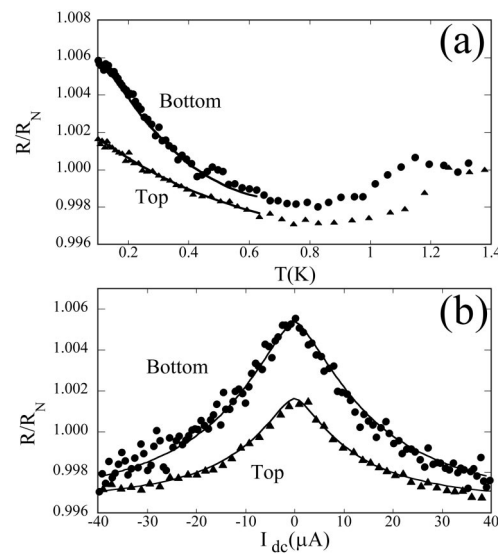


FIG. 2. (a) Resistance of top and bottom thermometers (normalized to the resistance R_N at $T = 1.2$ K) as a function of temperature. Solid lines are fits to Eq. (1) over the range 0.1–0.7 K. (b) Normalized differential resistance of top and bottom thermometer as a function of dc current through heater wire. Solid lines are fits to Eq. (2) over the range $I_{dc} = \pm 40$ μA , with the parameters $a = 2.1458$, $b = 0.46022$, $c = 40.348$ for the top thermometer, and $a = 4.3007$, $b = 2.5575$, $c = 62.362$ (with appropriate units) for the bottom thermometer. $R_N = 2.1537$ Ω for the top thermometer, and 4.3185 Ω for the bottom thermometer.

eters was measured using a homemade four-terminal low-frequency ac resistance bridge with an excitation current of ~ 500 nA, small enough to avoid self-heating, but large enough to measure without averaging for very long times. Figure 2(a) shows the normalized resistance R/R_N of both thermometers as a function of the temperature T as measured by the RuO₂ thermometer. As T is reduced, a drop in $R(T)$ is observed in both thermometers just below the transition temperature $T_c \sim 1.18$ K of the Al film. As T is lowered still further, the resistance increases, resulting in a minimum in $R(T)$ for both thermometers at $T \sim 0.8$ K. This nonmonotonic or reentrant behavior of $R(T)$ in mesoscopic proximity coupled normal metals is well known,^{8,9} and is a result of the spatial dependence of the electronic diffusion coefficient in the normal metal induced by its proximity to the superconductor. The overall change in resistance due to the proximity effect in our samples is $\sim 0.5\% - 1\%$, which is about a factor of 10 less than the expected resistance change for reentrant behavior in a nonmagnetic metal.¹⁰ We believe that this reduction is due to the presence of the implanted magnetic Fe impurities, which are expected to reduce the electron phase coherence length in the normal metal, and hence the amplitude of the proximity effect. Nevertheless, the magnitude of the resistance change is quite large. For example, the resistance contribution due to weak localization is typically on the order of 10^{-4} of the total resistance,¹¹ two orders of magnitude smaller than the temperature dependent resistance shown in Fig. 2.

In order to demonstrate the use of these thermometers to measure the local temperature of the electrons in the AuFe film, we flow a dc current I through the wide heater strip using the terminals marked $I_{dc} \pm$ in Fig. 1(a), while simultaneously measuring the resistance of both the top and bottom thermometers with an ac resistance bridge. The dc current

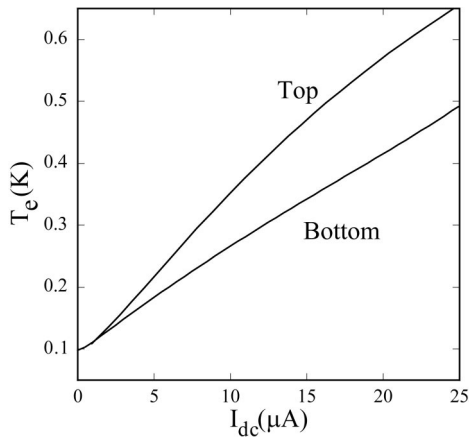


FIG. 3. T_e as a function of I_{dc} obtained by cross interpolating the fits for $R(T)$ and $R(I)$ shown in Fig. 2 for the top and bottom thermometer.

heats the electrons in the current path to a temperature above T_b . The electrons are cooled through interaction with phonons in the metal, and by electronic thermal conduction through the metallic parts of the sample itself, which is more efficient near the large contact pads of the sample. This leads to a nonuniform electron temperature profile in the heater wire.¹² Parts of the sample which are connected to the heater but do not have a dc current flowing through them (such as the reference wire) will also develop a temperature gradient as a function of the dc current through the heater.

Figure 2(b) shows the four-terminal ac resistance R of the top and bottom thermometer as a function of I . During this measurement, the mixing chamber of the dilution refrigerator was maintained at ~ 97.5 mK. Both curves are symmetric with respect to I , as would be expected since the heating of the electron gas by the dc current should be independent of the direction of the current. By correlating $R(I)$ shown in Fig. 2(b) with $R(T)$ shown in Fig. 2(a) for each thermometer, one can determine the effective electronic temperature at the node and at the contact pad of the reference wire as a function of I . In order to do this, we fit $R(T)$ for each thermometer to a fourth order polynomial of the form

$$R(T) = \sum_{j=0}^4 a_j (\log T)^j \quad (1)$$

over the temperature range of 0.07–0.625 K. The resulting fits are shown as the solid lines in Fig. 2(a). Similarly, $R(I)$ for both thermometers were fit by an equation of the form¹³

$$R(I) = a + \frac{b}{|I|^{3/2} + c} \quad (2)$$

as demonstrated by the solid lines in Fig. 2(b), which are fits to Eq. (2) over the range $I_{dc} = \pm 40 \mu\text{A}$. Finally, the effective electron temperature T_e as a function of I is obtained by cross interpolating between $R(T)$ and $R(I)$ obtained from the fits for each thermometer.¹⁴ Figure 3 shows $T_e(I)$ obtained in this manner for both thermometers. This plot indicates that even relatively small dc currents can substantially raise the effective temperature T_e over the bath temperature T_b . For example, at a dc current of $I \sim 5 \mu\text{A}$, T_e at the node is ~ 218 mK, an increase of ~ 120 mK over the bath tem-

perature of 97.5 mK. The electron temperature at the lower thermometer also increases substantially, to a value of 183 mK, giving a temperature differential of ~ 35 mK across the reference wire. These results correspond well with our numerical calculations using a model heat flow equation¹² at $I_{dc} < 10 \mu\text{A}$. At higher heating currents a large discrepancy is seen, which may be due to heating of the phonon gas which is not taken into account within this model. At lower temperatures, where cooling by phonons is less efficient, the heating effect would be expected to be even more drastic. These results underline the importance of using low excitation currents in low temperature transport measurements on mesoscopic samples in order to avoid self-heating of the electrons.

The use of Al as the superconductor in these thermometers restricts the temperature range of the thermometers to below ~ 0.6 K, but this range can easily be increased by using a superconductor with a higher T_c such as Pb or Nb. The ability to measure the spatial variation of the electron temperature that we have demonstrated here opens up the possibility of using these thermometers to make quantitative thermal and thermoelectric measurements on mesoscopic samples.

Support for this work was provided by the NSF through Grant No. DMR-9801982, by the David and Lucile Packard Foundation, and by the DOE-BES through Contract No. W-31-109-Eng-38.

¹H. Pothier, S. Guéron, N. O. Birge, D. Esteve, and M. H. Devoret, *Phys. Rev. Lett.* **79**, 3490 (1997).

²M. L. Roukes, M. R. Freeman, R. S. Germain, and R. C. Richardson, *Phys. Rev. Lett.* **55**, 422 (1985).

³R. A. Webb, R. P. Giffard, and J. C. Wheatley, *J. Low Temp. Phys.* **13**, 383 (1973).

⁴M. Henny, H. Birk, R. Huber, C. Strunk, A. Bachtold, M. Krüger, and C. Schönberger, *Appl. Phys. Lett.* **71**, 773 (1997).

⁵A. Mittal, R. G. Wheeler, M. W. Keller, D. E. Prober, and R. N. Sacks, *Surf. Sci.* **361/362**, 537 (1996).

⁶J. Eom, G. Neuttiens, C. Strunk, C. Van Haesendonck, Y. Bruynseraede, and V. Chandrasekhar, *Phys. Rev. Lett.* **77**, 2276 (1996); G. Neuttiens, J. Eom, C. Strunk, H. Pattyn, C. Van Haesendonck, Y. Bruynseraede, and V. Chandrasekhar, *Europhys. Lett.* **42**, 185 (1998).

⁷The samples were implanted at doses of 4×10^{12} and $4 \times 10^{13} \text{ cm}^{-2}$ at energies of 40 and 160 keV, respectively.

⁸P. Charlat, H. Courtois, Ph. Gandit, D. Mailly, and B. Pannetier, *Phys. Rev. Lett.* **77**, 4950 (1996).

⁹The resistance of our thermometers rises above the normal state resistance, unlike the samples in Ref. 8. The reason for this is unclear at present, but it may be due to repulsive electron–electron interactions in the normal metal.

¹⁰T. H. Stoof and Y. Nazarov, *Phys. Rev. Lett.* **76**, 823 (1996).

¹¹See, for example, B. L. Altshuler, A. G. Aronov, and D. E. Khmel'nitskii, "Coherent effects in disordered conductors," in *Quantum Theory of Solids*, edited by I. M. Lifshits (Mir, Moscow, 1982).

¹²The spatial dependence of the electron temperature can be described by a simple heat flow equation. See, for example, K. E. Nagaev, *Phys. Rev. B* **52**, 4740 (1995). The presence of leads attached to the center of the heater wire should have a strong heat sinking effect, creating a local minimum in the local electron temperature profile along the heater wire, which is taken into account in our numerical simulations.

¹³These functional forms [Eqs. (1) and (2)] were empirically determined to best describe the data with the fewest number of fitting parameters.

¹⁴For the bottom thermometer, the experimental $R(I)$ was offset by 0.002 Ω to match the zero bias resistance with the measured temperature dependent resistance at 97.5 mK before performing the analysis in order to account for an offset in the measurement.